The APPEA Journal 2018, **58**, 367–380
https://doi.org/10.1071/AJ17079

Peer reviewed paper

Using autonomous underwater gliders for geochemical exploration surveys

Louise M. Russell-Cargill[A], *Bradley S. Craddock*[A], *Ross B. Dinsdale*[A,B], *Jacqueline G. Doran*[A], *Ben N. Hunt*[A] *and Ben Hollings*[A]

[A]Blue Ocean Monitoring Ltd, Suite 3, Churchill Court, 234 Churchill Avenue, Subiaco, WA 6008, Australia.
[B]Corresponding author. Email: RDinsdale@BlueOceanMonitoring.com

Abstract. Offshore exploration commonly uses geochemical sniffer technologies to detect hydrocarbon seepage. Advancements in sniffer technology have seen the development of submersible in-situ methane sensors. By integrating a Franatech laser methane sensor onto an autonomous underwater glider platform, geochemical survey durations can be increased, and associated exploration costs reduced. This paper analyses the effectiveness of methane detection using the integrated system and assesses its practical application to offshore hydrocarbon seep detection methods. Blue Ocean Monitoring surveyed the Yampi Shelf, an area with known oil and gas accumulations, and observed hydrocarbon seeps on the North West Shelf of Australia. Results from the survey showed a background dissolved methane concentration of 3 to 4 volumes per million (vpm). A distinct plume of methane between 30 to 84 vpm measured over 24 km^2 was detected early in the survey. Three smaller plumes were also identified. Within a small plume, the highest concentration of methane was detected at 160 vpm. Methane above background levels was observed within 8 km of previously identified seeps; however, these seeps were unable to be pinpointed. Comparisons with data from previous surveys suggest similar oceanographic influences on the behaviour of the seeps, including tidal variations and the position of the thermocline. The results demonstrated that the integrated system may be used to effectively ground truth remote sensing interpretations and survey areas of interest over long durations, providing methane presence or absence results. To this effect, the integrated system may be implemented as a supporting technology for assessing the risks of further funding hydrocarbon detection surveys and focusing the area of interest before the deployment of vessel-based surveys.

Keywords: autonomous underwater gliders, autonomous underwater vehicles, autonomy, geochemical investigation, geochemical sniffers, glider integration, ground truthing, hydrocarbon seep, hydrocarbons, laser methane sensor, methane, natural seepage, oceanic methane layer, offshore technology, plumes, seep exploration surveys, Slocum Gliders, TDLAS, thermocline, tides, tunable diode laser absorption spectroscopy, Yampi Shelf.

Received 19 December 2017, accepted 1 February 2018, published online 28 May 2018

Introduction

Offshore exploration for oil and gas is an expensive and high-risk process with many investigations failing to identify economic hydrocarbon accumulations. Technologies that increase certainty in hydrocarbon accumulation identification and interpretation have the potential to reduce exploration risks. A study by Berge (2013) concluded that hydrocarbon seepage detection can initially indicate at least a partially functioning petroleum system. The study also suggests zero risk can be assumed for source presence, maturity and migration if an active seep is confirmed near a prospect, significantly reducing the overall risk of exploration. Numerous technologies exist to aid in the detection of seeps, and advancements in seep detection technology continue to evolve as the global demand for oil and gas pushes exploration efforts into deeper and more remote frontier basins.

Hydrocarbon seeps occur on the seafloor surface, producing variable mixtures of gases, liquids, solids, water, brine and mud (Berge 2013; Kinnaman *et al.* 2010; Sauter *et al.* 2006). The complex plumbing system of seeps, as described by Talukder (2012), have altering conduit systems that result in transient fluid flows that vary spatially and temporally. These seeps can be described as active or inactive, episodic or continuous (Abrams 2005). Hydrocarbon seepage can modify seafloor bathymetry, geochemistry and biology, often producing identifiable signatures such as carbonate crusts, hydrocarbon related diagenetic zones (HRDZ) and pockmarks (Hovland and Judd 1988).

The subsurface geology dictates the overall nature of the seep; however, seepage rates are also influenced by the sedimentary environment of the seabed, near-surface sediments, major direction of bulk flow, flux rate, concentration and the physical properties of the extruded material (Talukder 2012; and references therein). Short-term seepage expression and rates are also influenced by external factors that alter pore pressure and current direction, such as atmospheric pressure systems, storm surges, ocean swell, tides and bottom currents, which have been observed during seep surveys (e.g. Boles *et al.* 2001; Di *et al.* 2014; Stalvies *et al.* 2017).

Natural gases found at seep sites can be produced from biogenic or thermogenic origins, often surfacing as a combination of both (Schoell 1983, 1988). Traditional methods of determining the origin of natural gases require the use of gas chromatography (GC) and mass spectroscopy to calculate the bulk isotopic compositions of hydrogen and carbon, and proportions of methane to other hydrocarbons (Schoell 1980). Distinguishing between thermogenic and biogenic hydrocarbons is important in determining the probable source, where thermogenic methane is largely associated with the presence of mature oil and gas accumulations (Rice 1993).

Methane is commonly used to indicate the presence of hydrocarbon seeps because it is the main constituent in natural gas. The process by which methane fluxes from a seabed seep towards the atmosphere is largely unpredictable. The dissolution, microbial anaerobic oxidation and formation of methane hydrates, combined with oceanographic processes such as currents, upwelling and stratification, complicate the propagation and influence the overall residence time of the seep plume (Boetius *et al.* 2000; Kvenvolden 1995; Mau *et al.* 2007). To increase the likelihood of detecting seeps, technology that can maximise the temporal and spatial extent of an exploration survey is needed.

Hydrocarbon detection methods

Many petroleum reservoirs will have near surface hydrocarbon indicators, but not all survey methods are appropriate to detect them (Abrams 2005). Once a potential seep has been identified, three survey procedures are used to determine if hydrocarbon seepage is present in the subsurface or water column before exploratory drilling:

1) Remote sensing (airborne and spaceborne, active and passive).
2) Vessel-based geophysical survey (echo-sounder, multi-beam bathymetry, seismic profiling, side-scan sonar and sub-bottom profiler).
3) Vessel-based sampling (cameras, fluorometers, geochemical sniffers, remotely operated vehicles and sediment grabs).

Seep exploration commonly involves integrated studies using multiple survey methods to maximise the likelihood of detecting and correctly identifying a seep (e.g. Carragher *et al.* 2013; Hood *et al.* 2002). Remote sensing is often a cost-effective way to identify initial indicators of seepage in an area; however, results can often lead to false positives and require ground truthing (Fingas and Brown 2014; Logan *et al.* 2008). While vessel-based surveys are more effective in seep detection, they require coverage of large areas to target comparably small seeps, which can be inefficient and incur sizable survey costs. Autonomous systems that can be deployed before vessel-based surveys have the potential to confirm the presence of hydrocarbons in the water column, ground truth remote sensing interpretations and identify priority sampling areas, thus reducing vessel costs.

Geochemical sniffers

Where seeps are actively emitting hydrocarbons into the water column, geochemical sensors have the capability to detect relevant compounds. Traditionally, GC has been used to determine concentrations of gases in the water column by analysing water from a rosette sampler, or through pumping sea water from a towed fish to a laboratory onboard the vessel (Sigalove and Pearlman 1975). GC is still considered the superior method of hydrocarbon analysis because it provides high sensitivity and a range of measurements. However, it is also limited in its capabilities because the process can result in sampling artefacts and errors, and there are significant operational costs due to personnel and vessel resource requirements (Kamieniak *et al.* 2015).

The development of compact submersible membrane inlet mass spectrometers has resulted in sensors that provide detailed analysis of numerous dissolved gases in situ at high frequency and resolution (Chua *et al.* 2016). The system has had success in detection of hydrocarbons in the water column (e.g. Schlüter and Gentz 2008; Camilli and Duryea 2009), and can be integrated onto mobile and autonomous platforms (e.g. Camilli and Hemond 2004; Camilli *et al.* 2015); however, the weight, power requirements, availability and complexity of these sensors are still significant, and at the time of writing cannot be reasonably considered for long-term autonomous survey techniques.

The Franatech Aquaculture GmbH (Germany) laser methane sensor (LMS) has been developed using the principles of tunable diode laser absorption spectroscopy (TDLAS). In the past, TDLAS had been widely used for measuring atmospheric gas concentrations (e.g. Hovde *et al.* 1995; Wienhold *et al.* 1994). This submersible geochemical sensor measures dissolved methane concentrations, and provides higher resolution, sensitivity, accuracy and detection times (as outlined in Table 1) than comparable submersible methane sensors (Kamieniak *et al.* 2015). Comparable sensors such as the Franatech METS sensor (e.g. Bussell *et al.* 1999; Gasperini *et al.* 2012) may also experience erroneous readings as other gases can interfere with the instrument (Boulart *et al.* 2010). The lower power restrictions and lighter weight (Table 1) than the available membrane inlet mass spectrometers at the time of writing make the LMS the most suitable technology for long duration hydrocarbon surveys. The most significant issue with the LMS is that it cannot distinguish between biogenic and thermogenic methane, potentially resulting in false positives when applied to exploration. It is also limited in its capability to provide detailed analysis of any existing hydrocarbons because it is limited to the detection of methane concentration only.

Table 1. Franatech laser methane sensor specifications

Parameter	Range	Accuracy	Reaction times	Depth rating	Power consumption	Weight (in air)
Dissolved methane	2–10000 vpm[A]	± 0.9 vpm (range <150 vpm) ± 2.7% (range ≥150 vpm)	5 s 10 s (T90 time) 120 s (T99 time)	4000 m	5 W	10.6 kg

[A]Volumes per million.

Slocum Glider as a sniffer platform

Autonomous underwater vehicles (AUVs) can move passively using buoyancy or be actively propelled using a thruster. Passive AUVs have significantly lower energy requirements and, hence, have greater endurance than propelled vehicles. Actively propelled vehicles have previously been used to combine sampling and geophysical technology to increase efficiency and resolution in seep detection surveys, and have successfully integrated geochemical sensors into their payloads (e.g. Newman *et al.* 2008). However, the short duration (hours to days) and the operational expenses associated with the actively propelled AUVs, including vessel support, limit their applications to detect seeps by constraining the survey area and increasing project costs. Passive vehicles have longer endurance (weeks to months), and only require a vessel for deployment and recovery.

The Slocum G2 Glider (Glider) is a passively propelled AUV that operates on buoyancy principles. Originally proposed by Henry Stommel (Stommel 1989), further developments by Webb Research and Teledyne Webb Research have advanced Gliders into a diverse oceanographic survey platform. The Glider is manoeuvred through the water column by altering the internal volume, changing the buoyancy. It then acquires forward momentum due to two wings, producing a sawtooth shape profile through the water column. The Glider can also utilise a small thruster to produce variable dive profiles. The Glider uses dead reckoning to follow undulating trajectories set by a pilot based onshore, which are communicated to the Glider through Iridium satellite telemetry when on the surface.

Yampi Shelf survey site

The survey site on the Yampi Shelf was selected because it is one of few known seep fields in Australia with identified and measurable seepage (Logan *et al.* 2008). The Yampi Shelf is located within the Browse Basin on Australia's North-West Shelf (Fig. 1). Interest in the area began after the Gwydion-1 well (Spry and Ward 1997) and the Cornea Field (Ingram *et al.* 2000) proved that oil and gas accumulations were present. The Yampi Shelf has since been established as an active thermogenic seepage location, with multiple surveys confirming the presence of hydrocarbons.

Seismic acquisition and a geochemical survey gave initial evidence of active seepage on the shelf. Subsequently, a wide array of technologies were tested at this site to determine their detection capabilities. Six surveys over the Yampi Shelf have provided evidence of seeps over the area. The most notable datasets include:

- 1995: 2D Seismic data obtained in the Yampi Shelf Tie 2D Survey 165 (YST 165) by Australian Geological Survey Organisation (AGSO, now Geoscience Australia (GA)) (see O'Brien *et al.* 1996).
- 1996: GC data, including coverage of an area over the Yampi Shelf from the AGSO Marine Survey 176 (S176) (Wilson 2000).
- 2004: GA Survey 267 (S267), which provided a range of detection and identification instruments (see Jones *et al.* 2005).

S267 in 2004 trialled various technologies that are commonly used by oil and gas industry to detect seeps. These technologies included echo sounder, multi-beam swath bathymetry, towed fluorometer, acoustic Doppler profiler, underwater camera, submersible data logger, sediment cores, side-scan sonar, sub-bottom profiler and water samples. The geophysical data collected during YST 165 has also proven particularly important because it was required as supporting evidence of seepage measured by the other detection methods (Logan *et al.* 2008).

Logan *et al.* (2008) included a review of the main surveys and their techniques. Each technique was assessed and the abilities of each technology to detect seeps were analysed. All previously observed and imaged active seeps and HRDZ that are considered accurately identified by Logan *et al.* are summarised in Fig. 2. The locations of the active seeps identified were the basis of the sampling plan for this study.

Additional outcomes of these studies demonstrated the nature of the seeps on the Yampi Shelf and the external effects on seepage rates. Methane gas plumes in the water column were observed by echo-sounder and side-scan sonar. Plumes appear to rise 30 to 40 m from the seabed and are trapped at 40 to 60 m water depths along a stable thermocline (Rollet *et al.* 2006). The same study also showed the expression of the plumes is heavily influenced by high velocity currents and macro tidal cycles in the area. Plumes are also often associated with seafloor features such as pockmarks, HRDZ and mounds identified by swath bathymetry. The methane contour map produced from S176 also determined the spatial extent of dissolved methane on the Yampi Shelf (see Wilson 2000).

Given the cost and time advantages of long endurance autonomous systems used in exploration, the Glider is proposed as an effective platform to integrate a hydrocarbon detection sensor. The lighter weight, smaller power consumption and higher sensitivity of the LMS determined it as the most appropriate sensor to integrate onto the Glider. By conducting the survey in an area with prior evidence of methane seepage, the ability of the integrated system to successfully operate and detect methane can be determined. If effective, the Glider can provide a new long duration survey technique to detect the

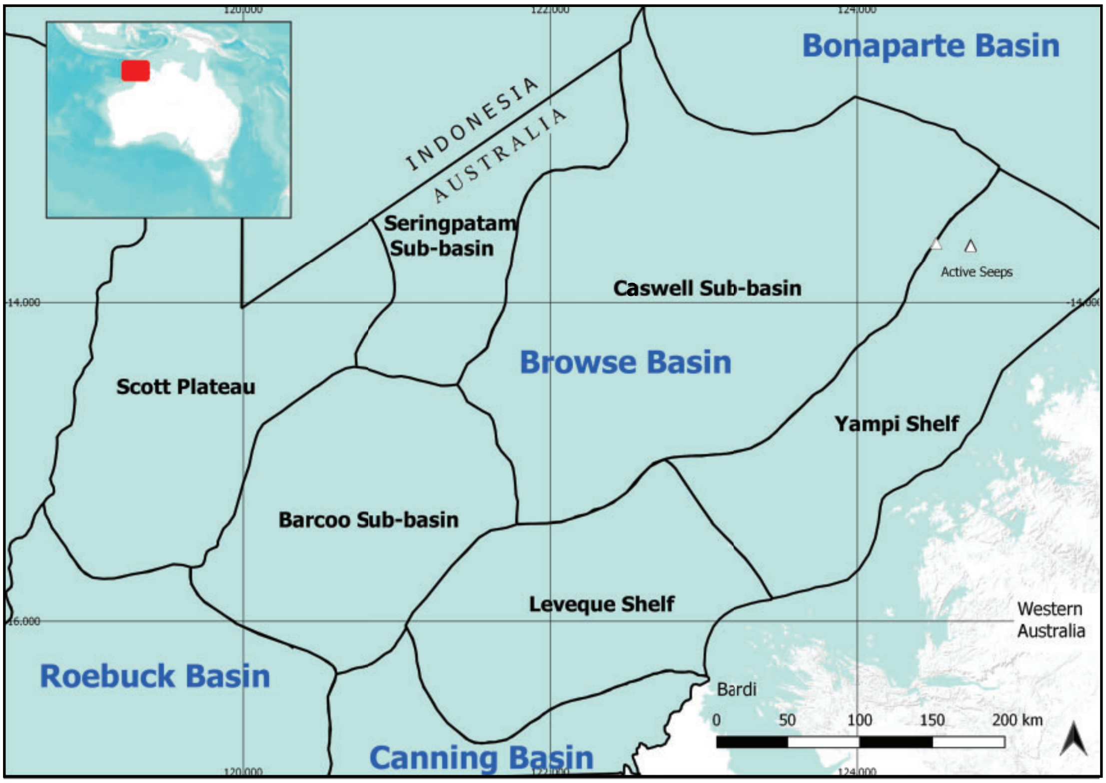

Fig. 1. Location of the active seeps and the Yampi Shelf respective to the Browse Basin on the Australian North-West Shelf. Geological provinces from Geoscience Australia (2017).

presence of methane concentrations above background. From this trial, the applications of this technology in commercial oil and gas industry can be assessed.

Methods

LMS integration

The LMS was electronically integrated into the Glider science bay and mounted on the underside of the hull (Fig. 3). A bracket was designed by Blue Ocean Monitoring Ltd (Blue Ocean) to hold the LMS parallel to the body of the Glider. A hemispherical nose cone was also mounted to the front of the LMS to improve hydrodynamics of the system. Collectively, the LMS, nose cone and mounting bracket weighed 12.34 kg in air. Due to the weight of the sensor, an extended bay section was included to create additional buoyancy. The additional weight and energy requirements of the LMS reduced the battery life, limiting the Glider survey to 17 operational days. The Glider was ballasted to target conditions on the Yampi Shelf estimated at 26.5°C, 34.6 PSU, and 1022.35 kgm^{-3}.

The LMS was calibrated by the manufacturer four months before deployment. Calibration values are outlined in Table 1. No internal modifications were made during integration of the LMS, ensuring the sensor remained in calibration.

Glider configuration

Additional sensors were installed into the Glider payload to determine the full capabilities of the integrated system in the detection of oil and gas seepage. These sensors included the LMS, Sea-Bird Electronics Glider Payload CTD, WET Laboratories SeaOWL UV-A fluorometer, Turner C3 fluorometer and the Aanderaa Oxygen Optode 4385. Detailed interpretations between methane concentrations and dissolved oxygen, fluorescence and salinity are beyond the scope of this article but may potentially have implications in future Glider geochemical studies.

The Glider used a standard G2 shallow 200 m buoyancy engine pump, enabling a maximum depth of 200 m, and lithium DD battery packs to maximise the Glider's endurance. The Glider was also equipped with an altimeter, tri-axial magnetic compass, pressure sensor, satellite global positioning system (GPS) and hybrid thruster. The compass and GPS are used to give WGS84-referenced latitude and longitude, pitch, roll and heading. Measurements of the Glider's heading, velocity and pitch were used to calculate a dead reckoned position while subsea. Depth averaged currents were inferred from the dead reckoned positions and surface GPS. Surface currents were estimated from multiple GPS fixes during surface drifts. The altimeter and pressure gauge were used to measure the water depth and depth of the Glider. A thruster was installed for additional propulsion in anticipation of high velocity currents on the shelf.

Field trial

The Glider was deployed on 23 July 2017 in the centre of the eastern active seeps where high methane concentrations were

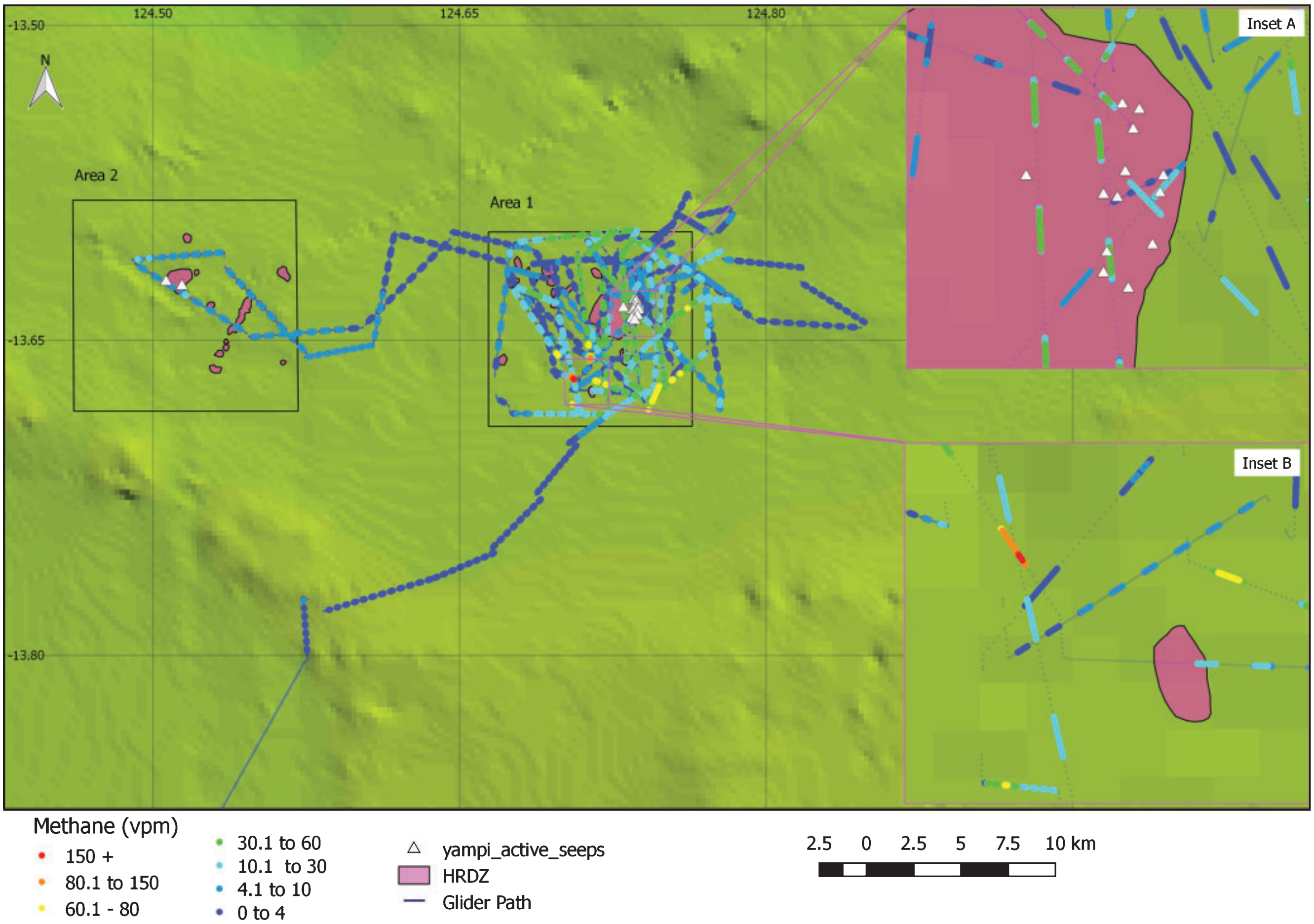

Fig. 2. Glider track over the Yampi Shelf showing methane concentration bins below 60 m water depth and locations of Area 1 and Area 2. HRDZ and active seeps from previous surveys have been summarised by Logan *et al.* (2008) and were provided by Geoscience Australia. Background concentrations occurred sporadically throughout the survey with little spatial correlation, but higher values are more localised near previously observed seeps. Inset map A shows greater detail of the Glider track around the previously observed seep sites. Inset map B shows a magnified area over the 160 vpm anomaly and 1 km proximity to the HRDZ.

expected. The Glider was recovered 50 km south-west of the deployment location on 5 August 2017, 17 days after deployment. The weather during this survey was typical for the north-west Australian dry season with no large-scale climate features effecting the area. Tidal information for the site was inferred from predicted tidal data supplied by the Australian Government Bureau of Meteorology (2017) for Heywood Shoals. Tidal range was expected to vary between 2 and 5 m.

During the survey, the Glider positioning and navigation were governed by locations of the active seeps, and local oceanographic conditions. A transect describes the Glider profiles and area between surfacing events. Sawtooth shape profiles are referred to individually as a yo. Bathtubs refer to profiles where the Glider is maintained at a predetermined depth over the entire transect. During the survey, yos were generally set to dive from 5 to 85 m water depth or 12 m above the seafloor, each taking ~15 to 20 min to complete. Bathtubs completed over the survey were maintained at a depth of ~85 m for 1.5 to 2.5 h, covering ~1.5 km. Battery position, thruster power, pitch and the pitch motor were adjusted throughout the survey to produce consistent profiles.

Waypoints were determined by the Glider pilots, based on potential seep locations and analysis of the depth-averaged currents measured by the Glider. The velocity of the depth-averaged currents ranged up to 0.5 m/s^{-1} or 1 kn throughout the survey. These currents were mostly tidally driven, switching from a south-east to north-west direction on a semi-diurnal basis. The Glider path was significantly influenced by the currents and an ideal 'lawnmower' survey pattern could not be obtained under these conditions. Instead, Glider paths were set to transect the general area of previously observed seeps. Limited time was dedicated to the sampling of the two western seep sites, allocating more time to investigate the higher density eastern seeps. Waypoints were set to manoeuvre the Glider up to 26 km south-west of the seeps to obtain background readings.

Data analysis

To quality control these data, a seventh order median filter was applied to the processed data to remove any spikes. Time series and profile plots were used to inspect the filtered data for overall data quality, suspect data and sensor faults, including sensor drift.

A time lag adjustment was also applied to these data to offset the time the sensor takes to output the equilibrated value. A correction of 90 s was applied because it produced the most probable methane concentration profile during the transects.

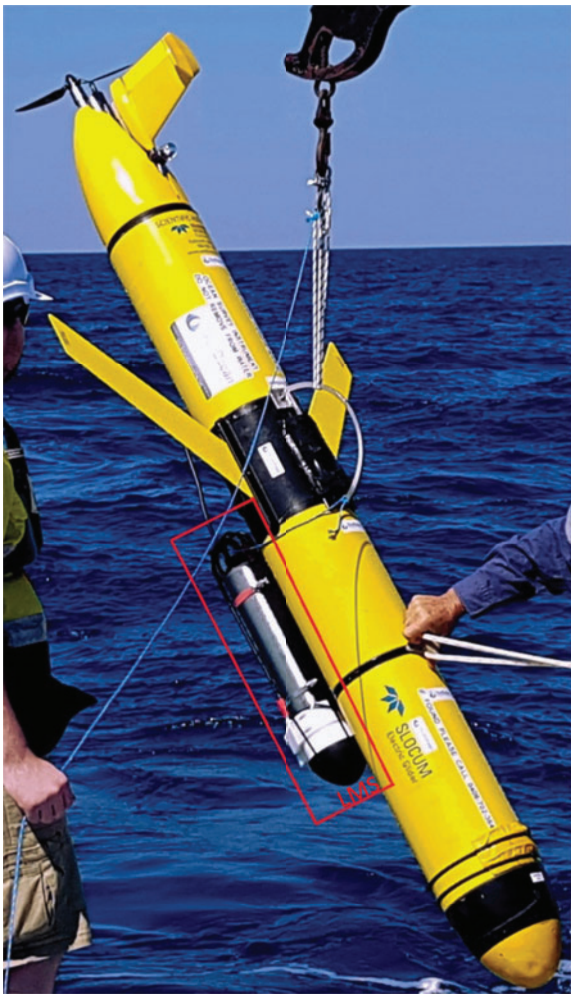

Fig. 3. Photograph of the Glider integrated with the LMS before deployment. The LMS is located inside the red outline.

Results

Using an arbitrary classification system, we describe high methane concentrations as more than 80 vpm, moderate as more than 30 vpm, and low as less than 30 vpm. The methane concentrations above 60 m were generally at background levels, so any discussion of methane concentrations are assumed as describing below 60 m depth unless stated. The methane values stated are excluding the sensor error margins outlined in Table 1.

Water column measurements taken 10 to 26 km to the south of the previously observed seeps ranged between 1 and 4 vpm. This confirmed that values below 4 vpm can reasonably be considered background concentrations in the area. These values are supported by S176 as background levels of 3 to 5 vpm were recorded in a similar location (Wilson 2000).

Over the 17-day survey, the Glider completed 637 yos and 12 bathtub profiles over 106 transects and collected over 400 km of transect data. Methane concentrations were detected between 0 and 160 vpm (Fig. 2). Where moderate to high concentrations were observed, there were very rarely background concentrations within the same transect.

Elevated methane concentrations generally occurred across multiple subsequent yos and covered large spatial extents, rather than sudden spikes (Fig. 4). This pattern was not observed at the thermocline; instead, a sharp change in methane concentration was observed at the thermocline, situated between 40 and 60 m (Fig. 5). An example of this trend is also observed in Fig. 4.

Area 1

The eastern seeps are covered by Area 1, as illustrated in Fig. 2. A range of concentrations were observed, from background to high level concentration. For 91 of the yos, moderate to high concentrations of methane were recorded; 14 of these yos detected methane concentrations above 60 vpm, and 2 above 80 vpm. These concentrations were measured within a 6.5 km radius of the seeps. All but one of the yos with concentrations of methane above 60 vpm occur to the south of the seeps.

The Glider passed within 250 m of the previously observed seeps during six transects (Inset A in Fig. 2). Concentrations recorded among the seeps varied between background and moderate levels. The two high concentration anomalies do not appear to be directly associated with these seeps, occurring 3.5 km and 4.8 km to the south-west.

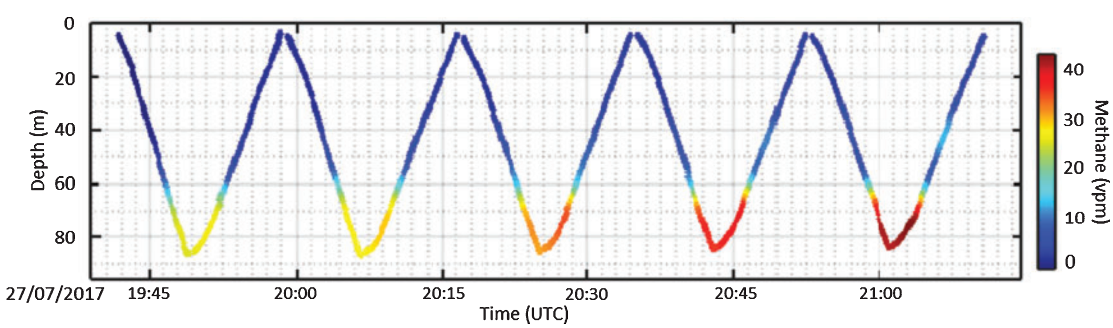

Fig. 4. An example of a transect showing the gradual changes in methane detection, and a comparatively abrupt change in methane concentration at 60 m depth.

Analysis of the yos within the 6.5 km radius of the previously observed seeps showed a reduction in the detection of methane over time. Of the 91 yos exhibiting moderate concentrations of methane, 74 were observed within the first 60 h of the survey. Measurements after this time show only 4% of yos recorded moderate concentrations, of which all were identified over 3 short periods.

Over a 17-h period on 23 and 24 July, the Glider circumnavigated the previously observed seep area within a 2 to 5 km radius, covering 26 km, and recorded peak methane

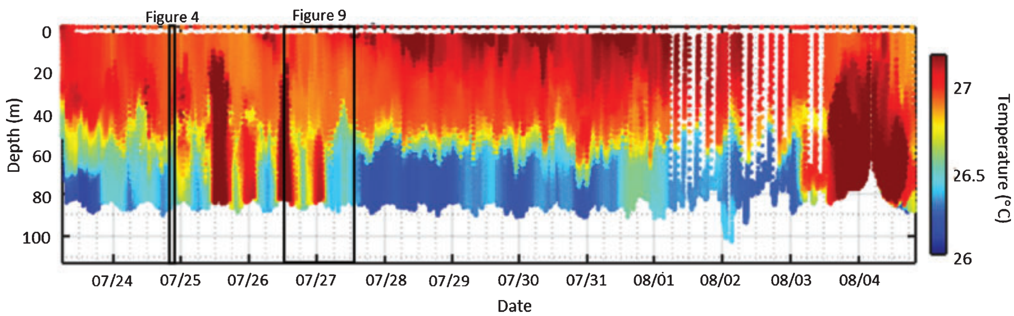

Fig. 5. Temperature depth data collected by the onboard CTD over the survey period. The temperature measurements confirm the depth of the thermocline at ~40 to 60 m. The period over which Fig. 4, and Fig. 9 is measured is also identified to illustrate the thermal environment of the yos.

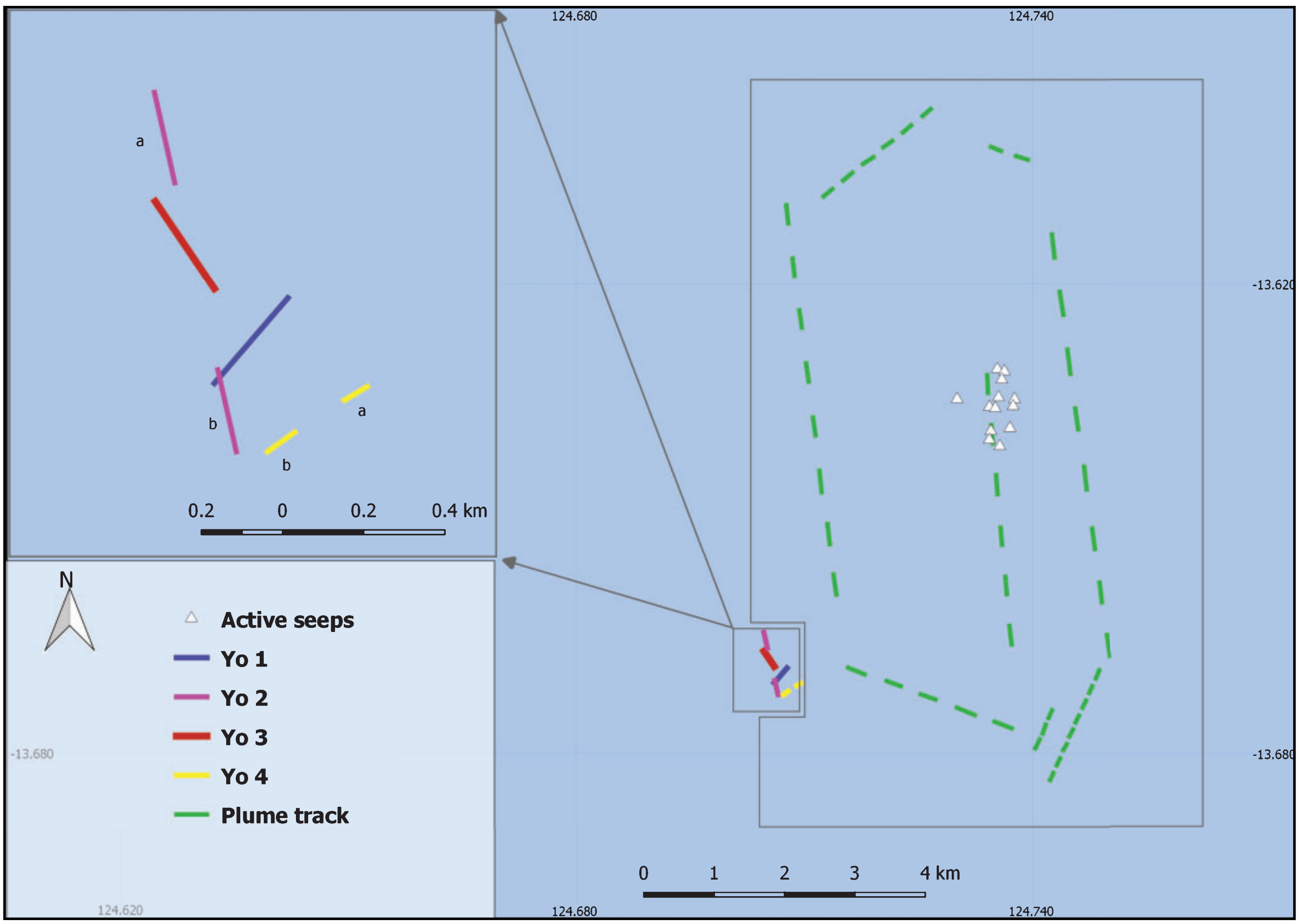

Fig. 6. The location of the plume track in relation to the previously observed seeps. The plume track includes values below 60 m where the maximum values of methane detected were consistently above 30 vpm for each yo. Also included are yos that were all obtained within the same area at the highest value (160 vpm), labelled in ascending time order. The inset shows the location of the yos in greater detail.

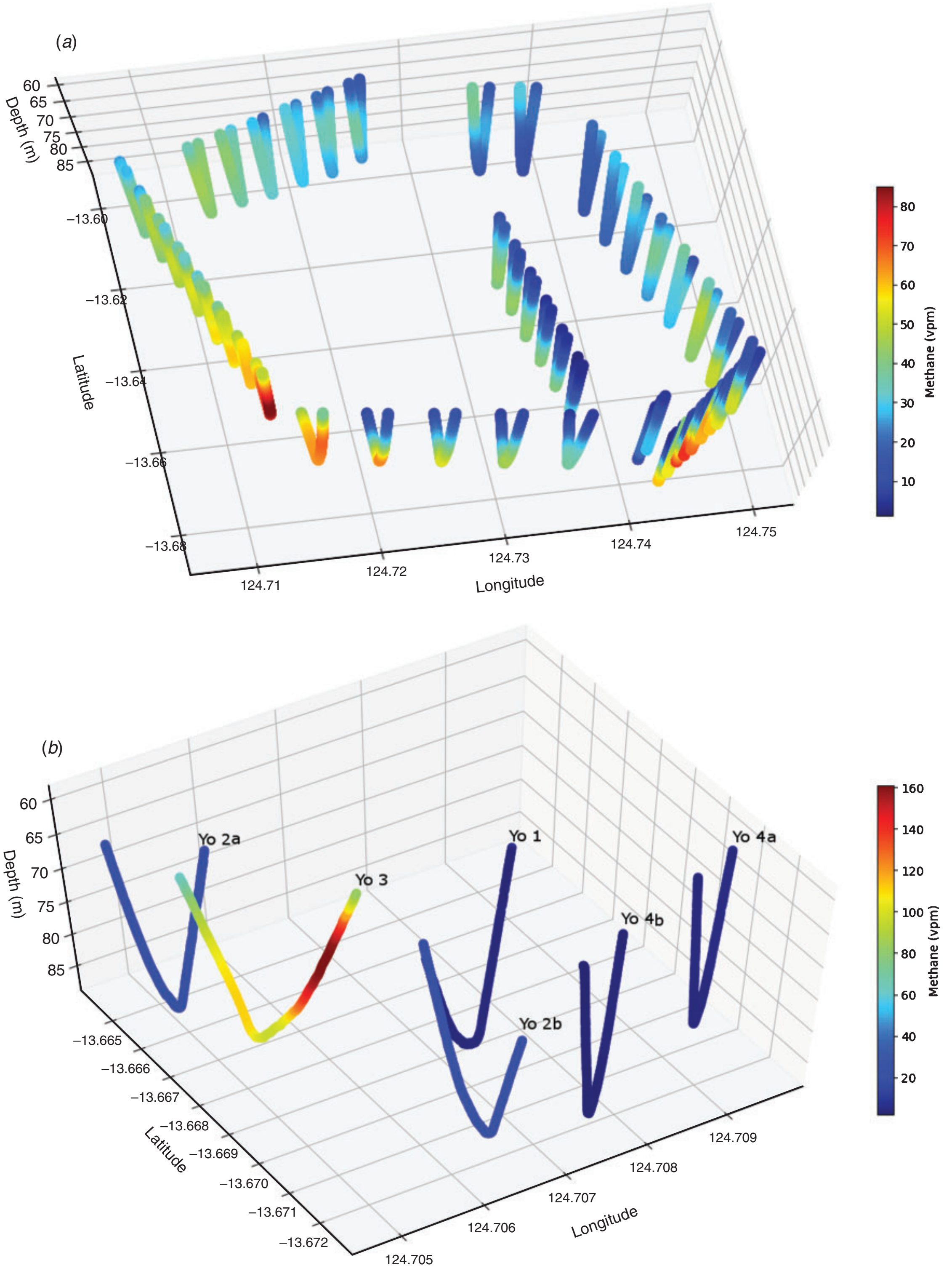

Fig. 7. (*a*) Three-dimensional view of the plume track. (*b*) Glider profile showing Yos 1 to 4 in a three-dimensional view. The highest methane concentration of 160 vpm is shown along Yo 3. Yo 2a and 2b measure maximum values of 25 vpm. Background values are seen on Yo 1, 4a and 4b.

concentrations of at least 30 vpm during each yo (see Fig. 6 and Fig. 7*a*). The second highest methane concentration for the survey was recorded 3.5 km to the south-west, at 84 vpm.

The highest concentration of 160 vpm (Fig. 8) was measured 5 km to the south-west of the previously observed seeps (Fig. 2). The high was recorded continuously for 20 s around 70 m depth.

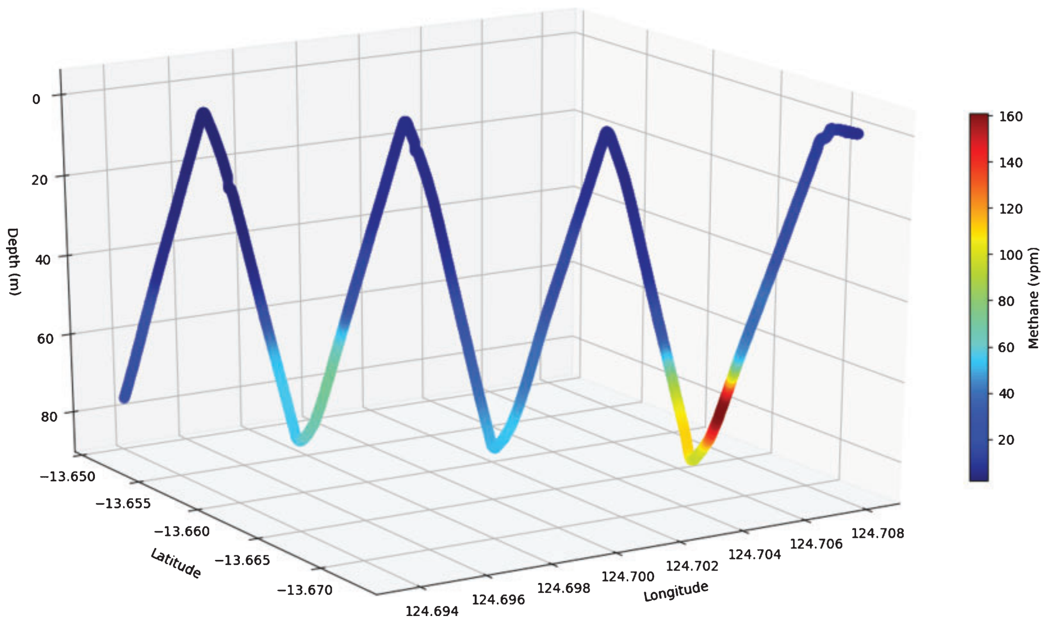

Fig. 8. Glider profile showing the three-dimensional view of the transect that intercepted the 160 vpm concentration.

This value was confined to one single ascent on the last yo of the transect and occurred 1 km north-west of a HRDZ observed during S267 (see Inset B in Fig. 2).

Three transects were completed near the 160 vpm anomaly within 24 h, with data from these transects illustrated in the inset in Fig. 6, and Fig. 7*b*. Background concentrations were observed during Yo 1, 4a and 4b, which were 300 m and 600 m away from the anomaly respectively. Both Yo 2a and 2b crossed the location of the anomaly at a shallower depth. Readings of 25 vpm were measured at the same depth of the anomaly 100 m to the north-west and 100 m to the south-east.

Area 2

Area 2 included the previously observed western seeps, as illustrated in Fig. 2. In general, the data showed slightly elevated concentrations of methane between 4 and 10 vpm. Higher values of 10 to 30 vpm were recorded over 3 yos within 2 km of the seeps. Limited ground was covered in the area.

It is worth noting that the concentrations of methane recorded during the transit between Area 1 and Area 2 were at background levels.

Discussion

During the trial of the system, the Glider was successfully piloted to survey the seep areas and collect high resolution data. Although periods of challenging oceanographic conditions were experienced, the Glider demonstrated the ability to operate efficiently with a sizeable external sensor payload attached.

Moderate concentrations measured in Area 1 over 23 to 24 July coincide with an area of moderate methane concentration observed through GC analysis during S176. The GC survey identified an area of ~310 km^2 with methane concentrations above 30 vpm, suggesting the presence of a significant seep plume. Because current directions were predominately north-west and south-east, it is likely that any dissolved methane plumes would be travelling further in these directions, resulting in an elliptical north-west and south-east trending plume. As the Glider survey was limited in the north-west and south-east directions, the extent of the plume may not have been fully surveyed. Further transects in these directions would have potentially mapped the full propagation of the plume, similar to that mapped during S176.

A correlation between higher methane concentration below the thermocline (Fig. 5) and lower concentrations above (e.g. Fig. 4) is consistent with the findings from Rollet *et al*. (2006). It is suggested that the thermocline may affect the concentrations by constraining the methane below this depth (Rollet *et al.* 2006). An exception occurred from 25 to 27 July, where the water column appears to have been warmer and well mixed, possibly a dense shelf water cascade (Pattiaratchi *et al.* 2011). This feature also coincided with a similar period of elevated methane concentration, suggesting the mixing event could have some influence on seepage expression. However, over this period the methane still appears to show the same concentration pattern. The presence of an oceanic methane layer, formed as bubbles dissolved at a certain depth (Leifer and Judd 2002), may provide an alternative explanation to this phenomenon, and was similarly proposed in the 2006 study by Rollet *et al*.

The peak 160 vpm measurement may indicate a new seep in the area, pinpointed by the integrated system. The typical seep profile observed over this anomalous high (Fig. 8) and relative proximity to a HRDZ (Fig. 2) suggests the data is not erroneous. However, due to a 3-h surface interval between the measured high (Yo 3) and the following yo, which resulted in a surface drift of 3 km, the quantity of data for interpretation of the peak measurement is limited. Further survey information is required to determine if it is a significant anomaly.

Focusing on the area surveyed within an 8 km radius of the previously observed eastern seeps, the general trend showed a decrease in the occurrence of elevated methane concentrations with time. This trend may be attributed to spring and neap tidal cycles, as the Glider was deployed just before the peak in the spring tide and recovered on the subsequent neap tide. During S267, methane plumes were identified as more active during spring tides and weakened during neaps, and a similar pattern was observed during the Glider survey. It is worth noting that a sampling bias towards the first 60 h of the survey may have affected the interpretation of these data. In this period, 147 yos were recorded within an 8 km radius of the eastern seeps, whereas only 293 yos and 10 bathtub profiles were recorded in the area over the next 348 h.

Four transects were acquired near the 160 vpm peak methane concentration, seen in Fig. 6 and Fig. 7*b*. Variations in methane measured in this area may be explained by various factors influencing seep expression. Tidal variations that significantly affect hydrostatic pressure are commonly attributed to changes in seep activity (e.g. Boles *et al*. 2001), and were previously attributed to seeps on the Yampi Shelf (Rollet *et al.* 2006) and regionally (Stalvies *et al.* 2017). Analysis of predicted tidal data suggests there is not a strong correlation between tidal changes and methane variation over this area (Fig. 9). This suggests tidal forcing alone is not responsible for methane venting from the sub-surface on the Shelf.

From examination of the Glider results, it is concluded that the previously observed seeps were not specifically identified. Moderate to high concentration of methane was observed during the Glider survey; however, these observations were not recorded above the location of the expected seeps. Given the complexity of the conduit systems and morphology of seeps, there are numerous explanations as to why the Glider may have been unsuccessful in detecting previously observed seeps.

The migration pathways of the seeps may have changed significantly over the 12 years since previously observed, and may be emanating further afield (Talukder 2012). The coarse-grained carbonate sediment features associated with the original seeps were relatively small because they were reworked by the high energy of the macrotidal environment (Rollet *et al.* 2006), suggesting possibly transient seeps in the area. It is also possible they have since been partially or fully blocked by reworking or microbial carbonate precipitation (Hovland 2002). The different climatic conditions, such as cyclonic low-pressure systems encountered during S176 and seasonal differences, may have also had a short-term influence on the expression of the seeps. Short-term temporal variations may have resulted in the Glider not passing previously observed seeps at the ideal time for observation, or alternatively the Glider may simply not have been positioned in enough proximity to the seeps to measure high values. Without reoccurring observations of higher methane concentrations in the locality of previously observed seeps, the ability of the Glider to pinpoint individual seeps cannot be guaranteed.

To this extent, future validations of the Glider system should use an area where seeps have more recently been identified and large tidal variations or current velocities are not present because piloting the Glider perfectly over a small seep is particularly challenging under these conditions. Using smaller yos at greater depths and more bathtub profiles may enhance the Glider's ability to pinpoint seeps and should be a main consideration in future seep survey plans. Some larger yos should still be incorporated into the survey plan because they were useful in validating the system and showing interesting seep characteristics that smaller yos may have missed.

Implications

The results of the survey suggest that the LMS-integrated Glider can be utilised to detect large dissolved methane plumes to determine the presence of active hydrocarbon seeps. The additional sensor payload enables the simultaneous collection of other relevant data. Because the LMS cannot differentiate between thermogenic or biogenic methane, there is no way to identify the original source of methane from these data alone. To this affect, the LMS-integrated Glider can be useful in studies

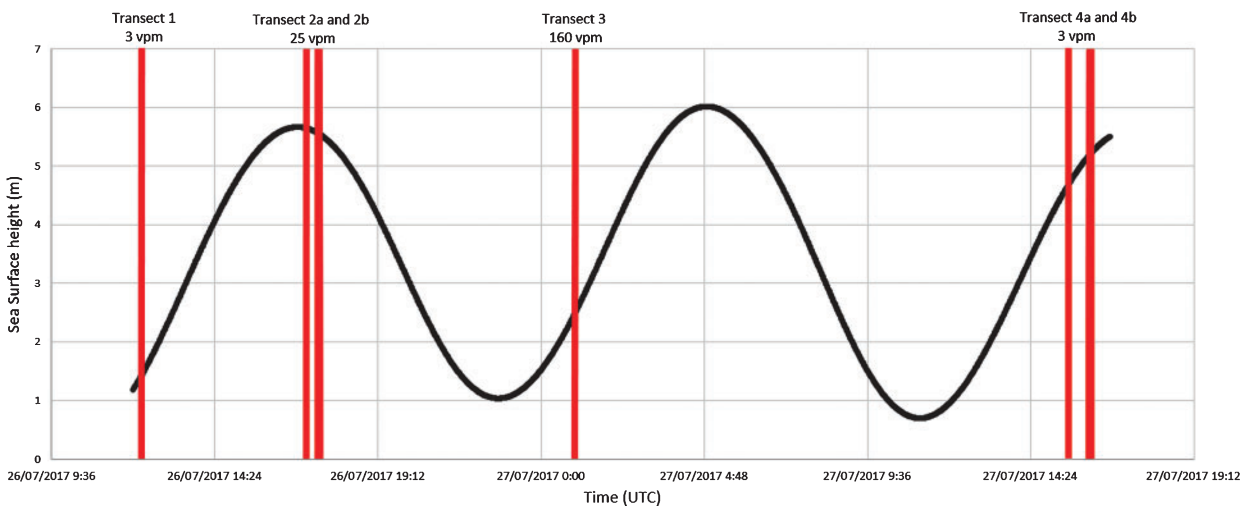

Fig. 9. Tidal estimates for Heywood Shoal over the survey duration (Australian Government Bureau of Meteorology 2017). The approximate timings of each yo (outlined in Fig. 6) in relation to the tidal height show methane concentrations relative to the cycle. Inverse relationships between tidal height and methane concentration are observed in Yo 2 and Yo 3; however, Yo 1 and Yo 4 do not appear to follow this trend.

investigating seep environments if further analysis or imaging of hydrocarbons is planned as a secondary method of identifying the presence of methane.

Given the low running costs of this platform, low health, safety and environmental risks, and real-time data collection, there is potential for this technology to be used specifically in oil and gas exploration. However, because it has not demonstrated a definitive ability to pinpoint seeps, we suggest the technology should be used to give a presence or absence methane survey to ground truth remote sensing data and focus the area of interest before deploying a research vessel utilising geophysical and geotechnical instrumentation. Deploying additional Gliders to operate in a 'swarm' would increase the likelihood of identifying a seep and improve the ability to track and image plumes in space (Petillo and Schmidt 2012).

Due to the large mass and power requirements of the LMS, the Glider's survey duration was not typical of a traditional Glider oceanographic survey and future improvements in system integration and battery life will allow for enhanced mission duration in seep survey applications.

Conclusion

The integrated LMS Glider system was used to survey the Yampi Shelf over the intended period and detected methane concentrations above background readings. The system was not able to identify the seeps observed in prior surveys; however, results showed elevated levels of methane within an 8 km radius of the observed seeps. The observations display evidence of physical oceanographic parameters acting on the methane plumes in a similar manner to those observed in a previous GA survey. Two anomalies measured by the Glider could indicate the presence of seeps not previously identified; however, without further supporting evidence this cannot be confirmed.

From the results of this survey, we conclude that the LMS Glider is a valid technology to aid in hydrocarbon detection, specifically oil and gas exploration. The system has proven capable of giving a methane presence or absence result; however, the full capability to locate seeps with precision is uncertain, and further testing over recently observed and consistent seeps is recommended. Advancements in Glider and sensor technology will further enhance capability to detect and map seeps, including the accuracy and resolution of captured data.

Conflicts of interest

This study was conducted and wholly funded by Blue Ocean. The survey was originally undertaken to determine if the hired LMS could be integrated and applied successfully to Gliders owned and operated by Blue Ocean. The survey results were scrutinised by senior company personnel to determine the validity of the integrated system and if it was a reliable asset with commercial applications. The company invested in the rental of the sensor and associated costs of the survey but did not fully invest in the technology until the survey demonstrated its capabilities, thus negating any financial conflicts of interest in data interpretation and representation. Blue Ocean has since purchased the sensor outright and intends to use it commercially.

Acknowledgements

The authors wish to acknowledge Walt McCall, Sam Ward and Nathan Kemp from Blue Ocean for the integration of the LMS and expert piloting of the Glider under difficult oceanographic conditions. We also extend our gratitude to GA for providing past survey data, figures and reports, and thank Dr Nadege Rollet for the ongoing support in survey planning and technical assistance during the research process.

References

Abrams, M. (2005). Significance of hydrocarbon seepage relative to petroleum generation and entrapment. *Marine and Petroleum Geology* **22**(4), 457–477. doi:10.1016/j.marpetgeo.2004.08.003

Australian Government Bureau of Meteorology (2017). Tide predictions, metadata and monthly sea level statistics. [Access: http://www.bom.gov.au/ntc/IDO59001/IDO59001_2017_WA_TP138.pdf]

Berge, T. B. (2013). Hydrocarbon Seeps: Recognition and Meaning. In 'Hydrocarbon seepage: From Source to Surface'. (Eds E. Amizadeh, T. B. Berge, and D. Connolly.) pp. 1–7. (Society of Exploration Geophysicists and American Association of Petroleum Geologists).

Boetius, A., Ravenschlag, K., Schubert, C. J., Rickert, D., Widdel, F., Giesecke, A., Amann, R., Jørgensen, B. B., and Pfannkuche, O. (2000). A marine microbial consortium apparently mediating anaerobia oxidation of methane. *Nature* **407**, 623–626. doi:10.1038/35036572

Boles, J. R., Clark, J. F., Leifer, I., and Washburn, L. (2001). Temporal variation in natural methane seep rate due to tides, Coal Oil point area, California. *Journal of Geophysical Research* **106**, 27077–27086. doi:10.1029/2000JC000774

Boulart, C., Connelly, D., and Mowlem, M. (2010). Sensors and technologies for in situ dissolved methane measurements and their evaluation using Technology Readiness Levels. *Trends in Analytical Chemistry* **29**(2), 186–195. doi:10.1016/j.trac.2009.12.001

Bussell, J., Klinkhammer, G., Collier, R., Linke, P., Appel, F., Heeschen, K., Erwin, S., De Angelis, M. A., Massom, M., and Marx, S. (1999). Application of the METS methane sensor to the in-situ detection of methane over a range of time scales and environments. In 'American Geophysical Union Fall Meeting, San Francisco, Dec 1999'.

Camilli, R., and Duryea, A. (2009). Characterizing marine hydrocarbons with in-situ mass spectrometry. *Environmental Science & Technology* **43**, 5014–5021. doi:10.1021/es803717d

Camilli, R., and Hemond, H. F. (2004). NEREUS/Kemonaut, a mobile autonomous underwater mass spectrometer. *Trends in Analytical Chemistry* **23**, 307–313. doi:10.1016/S0165-9936(04)00408-X

Camilli, R., Nomikou, P., Escartin, J., Rideao, P., Mallios, A., Kilias, S. P., and Argyraki, A. the Caldera Science Team(2015). The Kallisti Limnes, carbon dioxide accumulating subsea pools. *Scientific Reports* **5**, doi:10.1038/srep12152

Carragher, P. D., Ross, A., Roach, E., Trefry, C., Talukder, A., and Stalvies, C. (2013). Natural Seepage systems at Biloxi and Dauphini Domes and Mars Mud volcano, North East Mississippi Canyon Protraction Area, Gulf of Mexico. In 'Offshore Technology Conference, Texas, May 2013'. doi:10.4043/24191-MS

Chua, E. J., Savidge, W., Short, R. T., Cardenas-Valencia, A., and Fulweiler, R. W. (2016). A review of the emerging field of underwater mass spectrometry. *Frontiers of Materials Science* **3**, 209. doi:10.3389/fmars.2016.00209

Di, P., Feng, D., and Chen, D. (2014). Temporal Variation in Natural Gas Seep Rate and Influence Factors in the Lingtou Promontory Seep Field of the Northern South China Sea. *Terrestrial, Atmospheric and Oceanic Sciences Journal* **25**(5), 665–672. doi:10.3319/TAO.2014.04.30.01(Oc)

Fingas, M., and Brown, C. (2014). Review of oil spill remote sensing. *Marine Pollution Bulletin* **83**(1), 9–23. doi:10.1016/j.marpolbul.2014.03.059

Gasperini, L., Polonia, A., Del Bianco, F., Etiope, G., Marinaro, G., Favali, P., Italiano, F., and Çağatay, M. N. (2012). Gas seepages and seismogenic structures along the North Anatolian Fault in the eastern Marmara Sea. *Geochemistry Geophysics Geosystems* **13**(10), Q10018. doi:10.1029/2012GC004190

Geoscience Australia. (2017). Regional Geology of the Browse Basin. [Access: http://www.petroleum-acreage.gov.au/2017/geology/browse-basin/browse-basin-regional-geology.]

Hood, K. C., Gross, O. P., Wenger, L. M., and Harrison, S. C. (2002). Hydrocarbon systems analysis of the northern Gulf of Mexico: Delineation of hydrocarbon migration pathways using seep and seismic imaging. In 'Surface Exploration Case Histories: Applications of Geochemistry, Magnetics, and Remote Sensing'. (Eds D. Schumacher, L. A. LeSchack.) pp. 25–40. (American Association of Petroleum Geologists).

Hovde, C. D., Stanton, A. C., Meyers, T. P., and Matt, D. R. (1995). Methane emissions from a landfill measured by eddy correlation using a fast response diode laser sensor. *Journal of Atmospheric Chemistry* **20**, 141–162. doi:10.1007/BF00696555

Hovland, M. (2002). On the self-sealing nature of marine seeps. *Continental Shelf Research* **22**, 2387–2394. doi:10.1016/S0278-4343(02)00063-8

Hovland, M., and Judd, A. G. (1988). 'Seabed pockmarks and seepages. Impact on geology, biology and the marine environment.' (Graham and Trotman Ltd.).

Ingram, G. M., Eaton, S., and Regtien, J. M. M. (2000). Cornea case study: lessons for the future. *The APPEA Journal* **40**(1), 56–65. doi:10.1071/AJ99004

Jones, A. T., Logan, G. A., Kennard, J. M., O'Brien, P. E., Rollet, N., Sexton, M., and Glenn, K. C. (2005). Testing natural hydrocarbon seepage detection tools on the Yampi Shelf, north western Australia, Geoscience Australia Survey S267. Post Survey Report: GA Record 2005(15), 1–50.

Kamieniak, J., Randviir, E., and Banks, C. (2015). The latest developments in the analytical sensing of methane. *Trends in Analytical Chemistry* **73**, 146–157. doi:10.1016/j.trac.2015.04.030

Kinnaman, S., Kimball, J. B., Busso, L., Daniel, B., Ding, H., and Hinrichs, K. (2010). Gas flux and carbonate occurrence at a shallow seep of thermogenic natural gas. *Geo-Marine Letters* **30**(3–4), 335–365. doi:10.1007/s00367-010-0184-0

Kvenvolden, K. A. (1995). A review of the geochemistry of methane in natural gas hydrate. *Organic Geochemistry* **23**(11–12), 997–1008. doi:10.1016/0146-6380(96)00002-2

Leifer, I., and Judd, A. G. (2002). Oceanic methane layers: The hydrocarbon seeps bubble deposition hypothesis. *Terra Nova* **14**, 417–424. doi:10.1046/j.1365-3121.2002.00442.x

Logan, G. A., Jones, A., Ryan, G., Wettle, M., Thankappan, M., Grosjean, E., Rollet, N., and Kennard, J. (2008). Review of Australian Offshore Natural Hydrocarbon Seepage Studies. Geosciences Australia, Canberra.

Mau, S., Valentine, D., Clark, J., Reed, J., Camilli, R., and Washburn, L. (2007). Dissolved methane distributions and air-sea flux in the plume of a massive seep field, Coal Oil Point, California. *Geophysical Research Letters* **34**(22), L22603. doi:10.1029/2007GL031344

Newman, K. R., Cormier, M. H., Weissel, J. K., Driscoll, N. W., Kastner, M., Solomon, E. A., Robertson, G., Hill, J. C., Singh, H., Camilli, R., and Eustice, R. (2008). Active methane venting observed at giant pockmarks along the U.S. mid-Atlantic shelf break. *Earth and Planetary Science Letters* **267**, 341–352. doi:10.1016/j.epsl.2007.11.053

O'Brien, G. W., Blackburn, G., and Baird, J. (1996). Yampi Shelf Tie (YST) Basin Study and Interpretation Report: Yampi Shelf, Browse Basin, north western Australia. AGSO Record 1996, 60.

Pattiaratchi, C, Hollings, B, Woo, M, and Welhena, T (2011). Dense shelf water formation along the south-west Australian inner shelf. *Geophysical Research Letters* **38**, L10609. doi:10.1029/2011GL046816

Petillo, S., and Schmidt, H. (2012). *IFAC Proceedings Volumes* **45**, 232–237. doi:10.3182/20120919-3-IT-2046.00040

Rice, D. D. (1993) Biogenic gas: Controls, habitats, and resource potential. United States Geological Survey, Professional Paper (United States) **1570**.

Rollet, N., Logan, G. A., Kennard, J. M., O'Brien, P. E., Jones, A. T., and Sexton, M. (2006). Characterisation and correlation of active hydrocarbon seepage using geophysical data sets: An example from the tropical, carbonate Yampi Shelf, Northwest Australia. *Marine and Petroleum Geology* **23**(2), 145–164. doi:10.1016/j.marpetgeo.2005.10.002

Sauter, E. J., Muyakshin, S. I., Chalou, J., Schlüter, M., Boetius, A., Jerosch, K., Damm, E., Foucher, J., and Klages, M. (2006). Methane discharge from a deep-sea submarine mud volcano into the upper water column by gas hydrate-coated methane bubbles. *Earth and Planetary Science Letters* **234**(3–4), 345–365. doi:10.1016/j.epsl.2006.01.041

Schlüter, M., and Gentz, T. (2008). Application of Membrane Inlet Mass Spectrometry for Online and In Situ Analysis of Methane in Aquatic Environments. *Journal of the American Society for Mass Spectrometry* **19**(10), 1395–1402. doi:10.1016/j.jasms.2008.07.021

Schoell, M. (1980). The hydrogen and carbon isotopic composition of methane from natural gases of various origins. *Geochimica et Cosmochimica Acta* **44**, 649–661. doi:10.1016/0016-7037(80)90155-6

Schoell, M. (1983). Genetic characterization of natural gases. *AAPG Bulletin* **67**, 2224–2238.

Schoell, M. (1988). Multiple origins of methane in the Earth. *Chemical Geology* **71**(1–3), 1–10. doi:10.1016/0009-2541(88)90101-5

Sigalove, J. J., and Pearlman, M. D. (1975). Geochemical seep detection for offshore oil and gas exploration. In '7th Annual Offshore Technology Conference, Houston, May 1975'. pp. 95–100.

Spry, T. B., and Ward, I. (1997). The Gwydion discovery: a new play fairway in the Browse Basin. *The APPEA Journal* **37**, 87–104. doi:10.1071/AJ96005

Stalvies, C., Talukder, A., Ross, A., Emmanuelle, G., Carr, A., Williams, A., Gresham, M., Binning, M., and Jablonski, D. (2017). Establishing hydrocarbon charge to the Ashmore Platform, Bonaparte Basin, Australia: A natural seeps study. *Marine and Petroleum Geology* **82**, 56–68. doi:10.1016/j.marpetgeo.2016.12.018

Stommel, H. (1989). The slocum mission. *Oceanography* **2**(1), 22–25. doi:10.5670/oceanog.1989.26

Talukder, A. R. (2012). Review of submarine cold seep plumbing systems: leakage to seepage and venting. *Terra Nova* **24**(4), 255–272. doi:10.1111/j.1365-3121.2012.01066.x

Wienhold, F. G., Frahm, H., and Harris, G. W. (1994). Measurements of N_2O fluxes from fertilized grassland using a fast response tunable diode laser spectrometer. *Journal of Geophysical Research* **99**, 16557–16567. doi:10.1029/93JD03279

Wilson, D. J. (2000). AGSO Marine Survey 176 Direct Hydrocarbon Detection North-West Australia: Yampi Shelf, Southern Vulcan Sub-basin and Sahul Platform (July/September 1996) – Operational Report & Data Compendium. AGSO Record 200/42.

The authors

Louise Russell-Cargill completed her Bachelor of Science at the University of Western Australia, majoring in geology and marine science. Since graduating, Louise has gained field and research experience in offshore and onshore geology. She currently works concurrently for Blue Ocean Monitoring as a project support officer, and at CSIRO as a research technician.

Bradley Craddock is a systems engineer and data analyst currently working at Blue Ocean Monitoring. He holds a bachelor's degree in mechanical engineering from Curtin University and has over 10 years' experience as a business owner/manager, specialising in the design and development of prototype mechanical systems. He is also currently undertaking a master's degree in data science at the University of Western Australia.

Ross Dinsdale is the Asia Pacific General Manager for Blue Ocean Monitoring. Formerly, Ross was the Business Development Manager for an oil and gas exploration and production company, and he has also held investment banking and investment research roles in Australia and internationally covering the oil and gas sector. Ross is a Chartered Financial Analyst and holds a Bachelor of Commerce (UWA) and Graduate Diploma in Applied Finance (FINSIA).

Jacqui Doran has completed a Bachelor of Environmental Engineering, majoring in ocean systems engineering, and is currently pursuing her Master of Professional Engineering (Civil Engineering). Jacqui works for Blue Ocean Monitoring as a marine systems engineer, and has over four years' experience as an oceanographer.

Ben Hunt, the Chief Operations Officer at Blue Ocean Monitoring, obtained his bachelor's degree (with honours) in ocean science from the University of Plymouth. Ben has over 13 years' experience managing and leading team projects in various industries, including oil and gas, coastal engineering, mining and defence. He has extensive knowledge in geophysical, geotechnical, geochemical, environmental and metocean survey techniques. He has strong interests in physical oceanography, building of unmanned monitoring systems and deployment of disruptive technologies.

Ben Hollings finished his Bachelor of Engineering (and Commerce) in 2004, specialising in applied ocean science at the University of Western Australia. Ben is recognised globally as an expert in autonomous system development and implementation and operation of various vehicle types, and has been involved in various academic papers utilising AUVs. He has 10 years' experience working in remote ocean data collection using autonomous platforms including Sea Gliders and Slocum Gliders. He is currently the Group Chief Technical Officer at Blue Ocean monitoring, a leader in utilising autonomous underwater vehicles for ocean data collection.